


Article

Effect of Vinyl Flooring on the Modal Properties of a Steel Footbridge

Javier Fernando Jiménez-Alonso ^{1,*} , Jorge Pérez-Aracil ², Alejandro Mateo Hernández Díaz ² and Andrés Sáez ³

¹ Department of Building Structures and Geotechnical Engineering, Universidad de Sevilla, 41012 Sevilla, Spain

² Department of Civil Engineering, Catholic University of Murcia, 30107 Guadalupe (Murcia), Spain; jperez3@ucam.edu (J.P.-A.); amhernandez@ucam.edu (A.M.H.D.)

³ Department of Continuum Mechanics and Structural Analysis, Universidad de Sevilla, 41092 Sevilla, Spain; andres@us.es

* Correspondence: jfjimenez@us.es; Tel.: +34-954-556-602

Received: 10 March 2019; Accepted: 25 March 2019; Published: 1 April 2019



Abstract: Damping ratios associated with non-structural elements play an important role in mitigating the pedestrian-induced vibrations of slender footbridges. In particular, this paper analyses the effect of vinyl flooring on the modal parameters of steel footbridges. Motivated by the unexpected high experimental damping ratios of the first vibration modes of a real footbridge, whose deck was covered by a vinyl flooring, this paper aims at assessing more accurately the experimental damping ratios generated by this non-structural element on steel footbridges. For this purpose, a laboratory footbridge was built and vinyl flooring was installed on it. Its numerical and experimental modal parameters without and with the vinyl flooring were determined. The operational modal analysis method was used to estimate experimentally the modal parameters of the structure. The damping ratios associated with the vinyl flooring were obtained via the subtraction between the experimental damping ratios of the laboratory footbridge with and without the vinyl flooring. An average increase of the damping ratios of 2.069% was observed due to the vinyl flooring installed. According to this result, this type of pavement may be a useful tool to significantly increase the damping ratios of steel footbridges in order to reduce pedestrian-induced vibrations.

Keywords: non-structural damping; passive control; ambient vibration test; operational modal analysis; footbridges

1. Introduction

Modern footbridges are prone to vibrate under pedestrian-induced loading, due to two main factors: their first natural frequencies usually lie inside the frequency ranges which characterize the rhythmic human activities [1] and they usually exhibit low damping ratios [2]. Several examples have been reported in the literature about slender footbridges which have suffered from pedestrian-induced vibrations [3,4]. Two methods are usually used to control the vibratory response of slender structures under pedestrian action [2]: either (i) to modify the natural frequencies of the structure; or (ii) to increase the damping ratios of the structure (or both). The first method may be applied successfully during the design phase of the footbridge [5] or after its construction when the structural modifications are compatible with the aesthetic and functionality of the footbridge [6]. The second method is usually applied to existing structures or it can be also applied during the design phase if the slenderness of the structure makes impossible to control its response via the modification of either its stiffness or its mass [7].

The two usual options to increase the damping of a footbridge are [2]: (i) to take advantage of the damping introduced by non-structural elements; or (ii) to install external damping devices [8,9]. While the second option has been studied, analyzed and applied in numerous cases [10], the first option has received much less attention according to the best knowledge of the authors.

In this sense, the main motivation of this work is to shed some light on the use of non-structural elements as passive damping systems in order to reduce the pedestrian-induced vibrations in slender steel footbridges. The effective implementation of this alternative has two main advantages: (i) a smaller cost, when compared to the conventional external damping devices; and (ii) a better integration with the aesthetics of the footbridge.

This study was initially motivated by the unexpected high experimental damping ratios of a real footbridge, the Jorge Manrique footbridge (Murcia, Spain). This footbridge, a bowstring arch structure, suffered from comfort problems (falls of the users and pedestrian-induced vibrations) since its opening [11,12]. In order to improve the adherence of its deck and thus solve the problems of pedestrian falls, a vinyl flooring was installed on the structure. Unexpectedly, the placement of the vinyl flooring not only avoided falls among users but also reduced the pedestrian-induced vibrations. This last fact motivated the study of the effect of the vinyl flooring on the modal parameters of the structure. The modal parameters of the structure were identified experimentally and it was checked that the experimental damping ratios of the footbridge were unexpectedly higher than the values usually recommended by the most advanced design guidelines to assess the vibration serviceability of footbridges [13,14]. Due to the unexpected experimental damping ratios of this footbridge, the high vibration damping properties associated with vinyl polymers [15] and the growing practice of using vinyl flooring as pavements of footbridges [16], the authors decided to conduct a more detailed study on the effect of vinyl flooring on the damping ratios of steel footbridges.

In order to address this study and as it was not possible to remove the vinyl flooring of the Jorge Manrique footbridge due to service requirements, a laboratory steel footbridge with vinyl flooring was designed and built. A comparative method, successfully proposed by other authors to estimate the effect of non-structural partitions on the modal properties of floors [17], has been adopted herein to estimate the damping ratios associated with this non-structural element. The estimated damping ratios of the laboratory footbridge increased from an average value of 0.328% to a value of 2.397% after the vinyl flooring was installed.

The main outcome of the present study is the experimental assessment of the damping ratios generated by vinyl flooring when this non-structural element is used as the pavement of steel footbridges. An average non-structural damping ratio of 2.069% has been estimated experimentally. The results show that this type of pavement may be used as a valuable tool to increase the damping ratios of steel footbridges. Thus, vinyl flooring may be taken into account as a passive control system in order to mitigate the pedestrian-induced vibrations in slender footbridges. However, further studies are needed to better characterize the structural behavior of this non-structural element, making possible the development of mathematical models which allow predicting more accurately the response of steel footbridges damped with vinyl flooring; and to analyze in detail some reported limitations about the widespread use of these type of flooring in outdoor scenarios, such as, its strength to heavy point loads and the effect of sunlight exposure, the extreme temperatures and the defects of the subfloor on its structural behavior [18].

This paper is organized as follows. The main motivation of this study, a case study about the unexpected high damping ratios of the Jorge Manrique footbridge, is described in the second section. Subsequently, the main mechanisms which govern the generation of damping in footbridges and the description of the comparative method adopted herein to estimate experimentally the non-structural damping ratios associated with the vinyl flooring are presented in the third section. Later, both the estimation of the numerical and experimental modal parameters of a laboratory steel footbridge without and with the vinyl flooring and the experimental estimation of the damping ratios associated

with this type of pavement have been included in the fourth section. Finally, some concluding remarks are formulated to close the paper.

2. Unexpected High Experimental Damping Ratios of the Jorge Manrique Footbridge

In this section, the case study which motivated the development of this work is described in detail.

2.1. Description of the Structure, Numerical Finite Element (FE) Model and Numerical Modal Analysis

The Jorge Manrique footbridge is located at Murcia (Spain). It was designed and built to connect the two banks of the Segura River which crosses the urban center of this town. The footbridge is one of the most innovative bowstring arch footbridges built in Spain at the end of the last century (Figure 1a). Its structural system consists of two main tied-arches linked to a steel spatial truss deck by two groups of 48 inclined hangers with a diameter of 24 mm. The deck is isostatically supported on rolled and pinned bearings. The span of the footbridge is around 54 m. The deck has a variable width, from 12.9 m at the abutments to 6.4 m at mid-span. The depth of the deck is equally variable, evolving from 0.6 m at the abutments to 1.2 m at the mid-span. The cross-section of the upper arch is a steel tubular profile with a diameter of 350 mm and 40 mm of thickness. Finally, the steel truss deck is configured spatially by an upper grating composed by $\frac{1}{2}$ IPE-100 and HEA-100 European profiles and a spatial mesh of structural elements composed by tubular profiles whose diameter varies from 89 to 140 mm.



Figure 1. Jorge Manrique footbridge. (a) Longitudinal view of the structure and (b) view of the vinyl flooring installed on the footbridge.

The deck floor is composed of two layers: (i) a top vinyl non-woven flooring (Figure 1b) with 18 mm of thickness and a weight of 8.2 kg/m^2 [19] and (ii) a lower tempered glass layer with 30 mm of thickness. As mentioned previously, this upper layer was installed several years after the opening of the footbridge in order to avoid falls among pedestrians caused by its original sliding surface. During several years after its opening, local newspapers had published news about the complaints of the users due to both the falls and the high vibration level experienced when they crossed the footbridge [11,12]. Surprisingly the placement of the vinyl flooring not only improved the adherence of the floor but also the comfort level of the structure.

Thus, a study was performed to analyze the effect of this non-structural element on the modal parameters of the footbridge. The modal parameters of the structure were identified experimentally via signal processing, using an operational modal analysis (OMA) algorithm, of the measurements recorded during an ambient vibration test (AVT) [20]. In order to both establish the main parameters of this experimental test and check the experimental results, a finite element (FE) model of the footbridge was performed. The commercial FE analysis package Midas [21] was used for this purpose. The FE model was composed by 44,710 nodes and 58,192 elements. Two types of elements were considered: (i) 3D beam elements to model the arches and the deck and (ii) 3D cable elements to simulate the behavior of the hangers (Figure 2). For the FE model, it was assumed that the non-structural floor,

both the glass layer and the vinyl layer, does not modify the stiffness of the structure and only affects the mass. As mechanical properties of the steel, the values proposed by the European standards were adopted [22]: (i) density, $\rho_s = 7850 \text{ kg/m}^3$, (ii) Young's modulus, $E_s = 210000 \text{ MPa}$, and (iii) Poisson's ratio, $\nu_s = 0.3$. Finally, the footbridge is simply supported on four bearings. Each bearing is located at both sides of each arch.

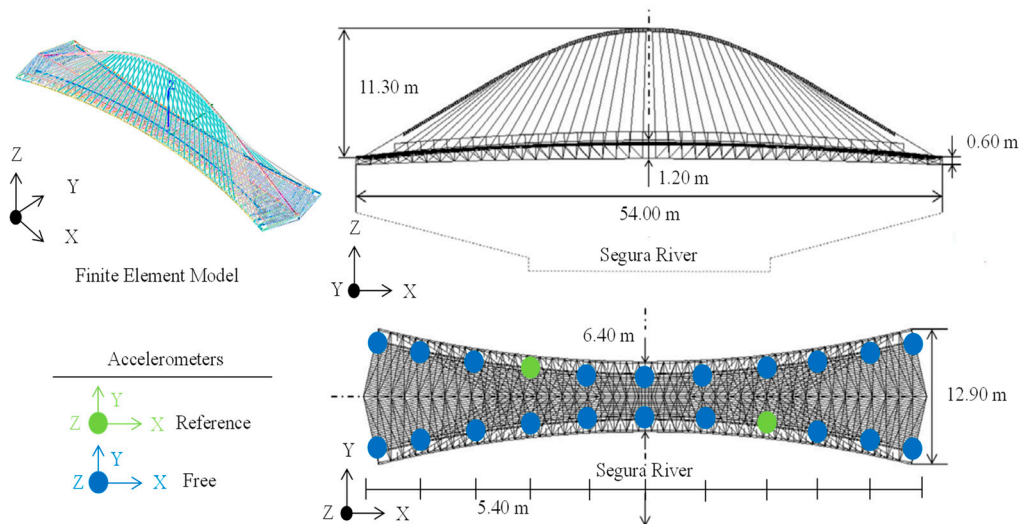


Figure 2. Description, finite element (FE) model and ambient vibration test (AVT) of the Jorge Manrique footbridge.

Two numerical FE modal analyses [23] were performed: (i) footbridge without the vinyl flooring and (ii) footbridge with the vinyl flooring. As results of these analyses the first three numerical vibration modes and associated numerical natural frequencies were obtained. Table 1 shows both the first three numerical natural frequencies without the vinyl flooring, $f_{num_wo,j}$, and with the vinyl flooring, $f_{num,j}$ (being j the number of the considered vibration mode). Additionally, Figure 3 illustrates the first three numerical vibration modes, $\phi_{num,j}$, of the Jorge Manrique footbridge with the vinyl flooring. As Table 1 shows the effect of the vinyl flooring on the numerical natural frequencies of this footbridge is low. The relative variations of the natural frequencies for the three considered numerical vibration modes are lower than 1.60% so this fact should not be the main cause of the modification of the comfort level of this footbridge.

Table 1. First three numerical natural frequencies without the vinyl flooring, $f_{num_wo,j}$, numerical natural frequencies with the vinyl flooring, $f_{num,j}$, experimental natural frequencies with the vinyl flooring, $f_{exp,j}$, experimental damping ratios with the vinyl flooring, $\zeta_{exp,j}$, relative differences with the vinyl flooring, $\Delta f_{exp,j}^{num,j}$, and modal assurance ratios with the vinyl flooring, $MAC_{exp,j}^{num,j}$, of the Jorge Manrique footbridge (being j the number of the considered vibration mode).

Modes	$f_{num_wo,j}$ [Hz]	$f_{num,j}$ [Hz]	$f_{exp,j}$ [Hz]	$\zeta_{exp,j}$ [%]	$\Delta f_{exp,j}^{num,j}$ [%]	$MAC_{exp,j}^{num,j}$ [-]	Description
1	0.785	0.774	0.828	2.68	-6.521	0.999	Lateral + Torsion
2	1.614	1.590	1.663	2.04	-4.389	0.998	Vertical
3	3.262	3.214	3.404	1.61	-5.581	0.951	Vertical

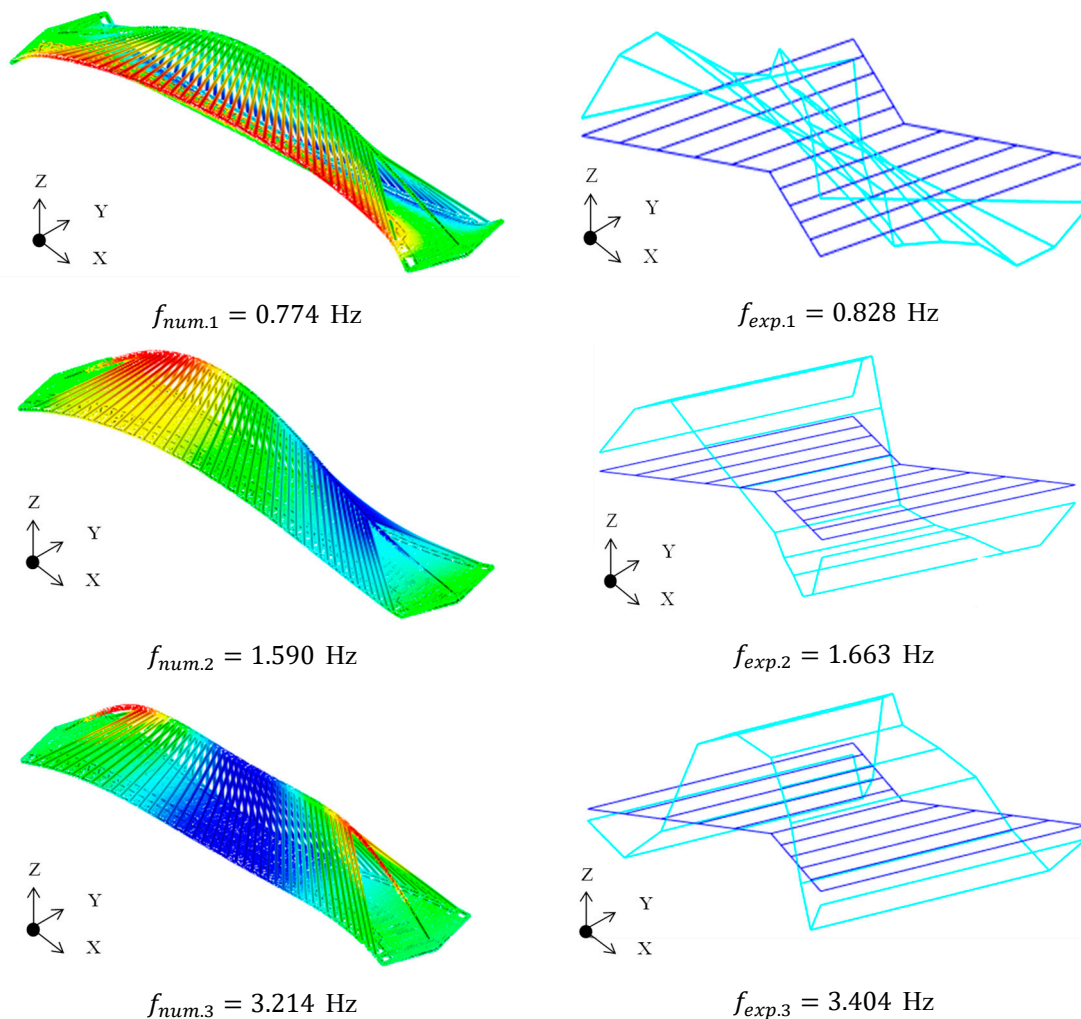


Figure 3. First three numerical, $\phi_{num,j}$, and experimental, $\phi_{exp,j}$, vibration modes of the Jorge Manrique footbridge with the vinyl flooring (being j the number of the considered vibration mode).

2.2. Experimental Identification of the Modal Parameters of the Jorge Manrique Footbridge

Subsequently, an AVT was performed to identify experimentally the modal parameters of the structure. The experimental test was conducted under ambient conditions. The response of the structure under ambient excitation was measured along two gridlines located on each lateral edge of the deck (Figure 2). As a data acquisition system, the Kinematics Granite equipment was considered. A total of 2×11 points equally distributed along each longitudinal alignment were instrumented. Three high sensitivity triaxial force balance accelerometers (Kinematics Episensor ES-T, Pasadena, US) were used. Two of these devices were established as references, and the other one was moved successively to the different positions of the gridlines. An optimal sensor placement algorithm [24] was used to select the best location for the two reference accelerometers. The considered locations ensure the identification of all the vibration modes whose natural frequencies were inside the range that characterizes the pedestrian-structure interaction phenomenon [13,14]. Twenty different set-ups were conducted during this AVT. The parameters required to conduct this AVT were determined based on the results of the previous numerical modal analysis. Thus, a sampling frequency of 100 Hz and duration for each set-up of 600 s were considered.

In order to identify the experimental modal parameters of the footbridge, the signals recorded during this AVT were processed via an OMA algorithm. The stochastic subspace identification (SSI) method [20] was considered herein due to its greater accuracy for the estimation of the damping ratios of the structure [25]. This identification method is implemented in the software package

Artemis [26], which has been used herein. Thus, the first three natural frequencies and associated vibration modes were identified experimentally. Table 1 shows the first three experimental natural frequencies, $f_{exp,j}$ (being j the number of the considered vibration mode), and Figure 3 illustrates the first three experimental vibration modes, $\phi_{exp,j}$, of the Jorge Manrique footbridge.

The obtained numerical and experimental natural frequencies and vibration modes are compared in Table 1. In order to validate the correlation between the numerical and experimental modal parameters both the relative differences, $\Delta f_{exp,j}^{num,j}$, between each considered numerical and experimental natural frequency j and the modal assurance criterion ratios, $MAC_{exp,j}^{num,j}$, between each considered numerical and experimental vibration mode j were analyzed [27].

The relative difference, $\Delta f_{exp,j}^{num,j}$, between a numerical and experimental natural frequency j may be expressed as:

$$\Delta f_{exp,j}^{num,j} = \frac{f_{num,j} - f_{exp,j}}{f_{exp,j}} \Delta 100 \text{ [%]} \tag{1}$$

where $f_{num,j}$ is the numerical natural frequency [Hz] and $f_{exp,j}$ is the experimental natural frequency [Hz] of the vibration mode j .

The modal assurance criterion, $MAC_{exp,j}^{num,j}$, between a numerical and experimental vibration mode j may be defined as:

$$MAC_{exp,j}^{num,j} = \frac{(\phi_{num,j}^T \Delta \phi_{exp,j})^2}{(\phi_{num,j}^T \Delta \phi_{num,j}) \Delta (\phi_{exp,j}^T \Delta \phi_{exp,j})} [-] \tag{2}$$

where $\phi_{num,j}$ and $\phi_{exp,j}$ are respectively the numerical and experimental vibration modes to be compared and T denotes the transpose. A good correlation between two vibration modes is achieved when the value of its $MAC_{exp,j}^{num,j}$ ratio is greater than 0.90 [27].

As Table 1 shows both the value of the experimental natural frequencies and associated vibration modes are in good agreement with the results obtained numerically. The relative differences, $\Delta f_{exp,j}^{num,j}$, were inside the usual variation range predicted during the design phase of a footbridge [28], and all the $MAC_{exp,j}^{num,j}$ ratios are greater than 0.90.

At this point, it is necessary to highlight two facts: (i) although the natural frequencies of the structure are inside the frequency ranges which characterize the human rhythmic action [13,14] and the pedestrian traffic on the footbridge is high no vibratory problems have been reported in this footbridge after the installation of the vinyl flooring; and (ii) the experimental damping ratios, $\zeta_{exp,j}$ (being j the number of the considered vibration mode), of the three identified vibration modes are clearly greater than the usual values recommended by the most advances design guidelines (Table 2).

Table 2. Damping ratio, ζ_j , recommended by different design guidelines [13,14] being j the number of the considered vibration mode.

Construction Type	Damping Ratio, ζ_j , [%]					
	French Guidelines [13]			European Guidelines [14]		
	Serviceability Conditions		Large Vibrations	Serviceability Conditions		Large Vibrations
	Minimum	Mean	Mean	Minimum	Mean	Mean
Reinforced concrete	0.80	1.30	5.00	0.80	1.30	5.00
Prestressed Concrete	0.50	1.00	2.00	0.50	1.00	2.00
Steel welded joints	0.20	0.40	2.00	0.20	0.40	2.00
Steel bolted joints	0.20	0.40	4.00	0.20	0.40	4.00
Composite	0.30	0.60	-	0.30	0.60	-
Timber	1.50	3.00	-	1.00	1.50	-
Stress-ribbon	-	-	-	0.70	1.00	-

As the unique modification performed on the footbridge during its overall life cycle was the installation of the vinyl flooring, it was assumed that the improvement of its comfort level was caused by this fact. Additionally, as it was checked that the modification of the natural frequencies of the footbridge due to the presence of the vinyl flooring was small (Table 1), it was assumed that the main effect of the vinyl flooring on the footbridge was the increase of its damping ratios. Thus, the experimental verification of this assumption motivated the development of this study.

In the next section, an overview of the different mechanisms that generate damping in civil engineering structures is included. Additionally, the comparative method considered herein to estimate experimentally the effect of vinyl flooring on steel footbridges is described in detail.

3. Viscous Damping Mechanisms for Vibrating Footbridges

Real footbridges dissipate energy when they vibrate according to different mechanisms. The energy dissipated during the vibratory process may be determined as the sum of the simultaneous actuation of all these mechanisms [29]. According to their fundamental mode of energy dissipation, damping mechanisms may be classified in three groups [30]: (i) dissipation within a solid (material damping); (ii) dissipation within or to a fluid medium (fluid damping); and (iii) dissipation at the interfaces between solids (friction damping). The material damping mechanism refers to the inherent energy dissipation process which converts its kinetic energy to thermal energy during each cyclic deformation. The fluid damping mechanism refers to both the energy lost from a vibrating surface through wave radiation (radiation damping) and the energy lost through drag forces on a solid body moving in a fluid (drag forces damping). Finally, the friction damping mechanism refers to the dissipation process in which mechanical energy is transformed into heat during each cyclic motion [30].

In order to model mathematically these dissipative mechanisms, several damping models have been proposed [31]. In general, for linear systems, these damping models may be classified into two groups: (i) viscous damping models and (ii) non-viscous damping models. In the viscous damping models, the damping forces do not depend on the past history of the motion of the structure, whereas in the non-viscous damping models, the damping forces are strongly dependent of the previous behavior of the structure. Thus, due to its simplicity and better computational behavior, viscous damping models have been widely used. In fact, viscous damping models have been adopted by the most advanced design guidelines [13,14]. Such viscous damping models are characterized by the damping ratio, ζ_j (being j the number of the considered vibration mode), which is defined as the ratio between the damping coefficient and the critical damping coefficient [23].

In this manner, the overall damping ratio of civil engineering structures, ζ_j , may be expressed in terms of the different dissipative elements involved as follows [32]:

$$\zeta_j = \zeta_{s,j} + \zeta_{ns,j} + \zeta_{a,j} + \zeta_{d,j} \quad (3)$$

where

$\zeta_{s,j}$ is the structural damping ratio (associated with the structural elements) [%].

$\zeta_{ns,j}$ is the non-structural damping ratio (associated with the non-structural elements) [%].

$\zeta_{a,j}$ is the aerodynamic damping ratio (associated with the air-structure interaction) [%].

$\zeta_{d,j}$ is the special devices damping ratio (associated with installed external damping devices as tuned mass dampers, sloshing tanks, etc.) [%].

Although there are some design guidelines—as for instance the European standard [32] to check the vibration serviceability limit state of building under wind action, which allow an accurate estimation of the damping ratio in terms of its different dissipative elements—in the case of footbridges, only overall damping ratios are provided by the most advanced design guidelines [13,14]. Table 2 shows the values recommended by these design guidelines in terms of the construction type and the level of vibrations. The values provided by Table 2 are conservative and do not allow estimating the value of the damping ratio of a particular footbridge in terms of its actual design.

In order to overcome this limitation, in this study the effect of a non-structural element, the vinyl flooring, on the damping ratios of steel footbridges is analyzed experimentally. As it was not possible to conduct experimental tests on the Jorge Manrique footbridge, given that its service had to be maintained, a laboratory steel footbridge was built for this purpose.

A comparative method, previously applied successfully to determine the effect of partitions on the modal properties of floors [17], was considered herein to estimate experimentally the effect of the vinyl flooring on the damping ratios. According to this method, the non-structural damping ratios generated by this type of pavement may be estimated by comparing the experimental damping ratios of the structure obtained under two different scenarios: (i) footbridge without the vinyl flooring and (ii) footbridge with the vinyl flooring. The estimation of the experimental damping ratios has been performed via the application of an operational modal analysis (OMA) algorithm in the time domain [25]. It was assumed that the experimental damping ratios identified under ambient vibration conditions correspond to a combination of two dissipative mechanisms, material and frictional damping.

4. Assessment of the Dynamic Behavior of a Laboratory Footbridge without and with the Vinyl Flooring

In this manner, a laboratory steel footbridge was built and its experimental modal parameters were estimated based on the mentioned comparative method. In the next sub-sections, the identification process is described in detail.

4.1. Description of the Structure, Numerical FE Model and Numerical Modal Analysis

The laboratory footbridge is a frame steel structure (Figure 4). The structure has only one span of about 4 m of length. The deck is composed by two longitudinal lateral beams and five transverse beams. The cross-section of the longitudinal beams is a European profile UPN 50 × 25 × 5 mm. The transverse beams are configured by two different profiles: (i) for the transverse beams at the supports, a single L 50 × 5 mm profile is considered and (ii) for the remaining transverse beams, a double L 50 × 5 mm profile is chosen. Four columns, UPN 50 × 25 × 5 mm, link the deck of the structure to the foundation. Additionally, a tramex panel (30 × 3 mm) is included between each two transversal beams. The columns are clamped to the foundation slab and simply pinned to the deck. The vinyl flooring was installed on the footbridge mimicking the same connection conditions of the Jorge Manrique footbridge. The vinyl flooring was connected to the laboratory footbridge via several steel clamps. The clamps were separated longitudinally around 0.5 m and transversally around 0.8 m.

A FE model of the structure was built (Figure 4) with the FE package Midas [21]. A numerical model with 133 nodes and 156 elements was developed in order to both assist in the design of the subsequent AVT test and check the experimental modal parameters. Two types of elements were used to build this numerical model: (i) 3D beam elements and (ii) 3D shell elements. In this manner, the behavior of all the beams and columns of the structure were simulated by the 3D beam elements. Meanwhile, the 3D shell elements were considered in order to simulate numerically the behavior of the tramex panels. A linear isotropic constitutive law was considered for 3D beam elements while a linear orthotropic constitutive law was taken into account for the 3D shell elements. As material properties for the steel, the values recommended by European standards were again chosen [22]. As an assumption, the effect of the vinyl flooring was simulated again via the modification of the mass matrix of the structure by an equivalent distributed mass of 8.2 kg/m² [19].

Subsequently, the numerical natural frequencies of the laboratory footbridge for the two different scenarios were obtained through two different numerical modal analyses [23]. Thus, the first five numerical vibration modes of the footbridge without, $f_{num,j}^{wo_vf}$, and with, $f_{num,j}^{w_vf}$, the vinyl flooring (being j the number of the considered vibration mode) are shown in Table 3. Additionally, Figures 5 and 6 illustrate the first five numerical vibration modes of the laboratory footbridge without, $\phi_{num,j}^{wo_vf}$, and with, $\phi_{num,j}^{w_vf}$, the vinyl flooring respectively.

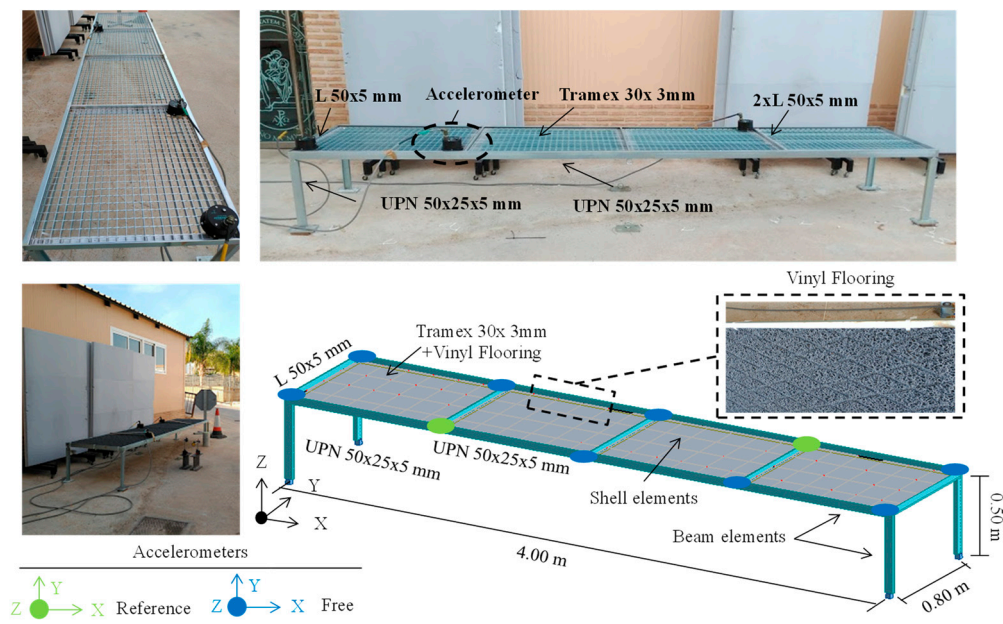


Figure 4. Description, FE model and AVT of the laboratory footbridge.

Table 3. First five numerical natural frequencies, $f_{num,j}^{wo_vf}$ and $f_{num,j}^{w_vf}$, experimental natural frequencies, $f_{exp,j}^{wo_vf}$ and $f_{exp,j}^{w_vf}$, experimental damping ratios, $\zeta_{exp,j}^{wo_vf}$ and $\zeta_{exp,j}^{w_vf}$, relative differences, $\Delta f_j^{wo_vf}$ and $\Delta f_j^{w_vf}$, and modal assurance criterion ratios, $MAC_j^{wo_vf}$ and $MAC_j^{w_vf}$, of the laboratory footbridge without and with the vinyl flooring (being j the number of the considered vibration mode).

Modes	$f_{num,j}^{wo_vf}$ [Hz]	$f_{num,j}^{w_vf}$ [Hz]	$f_{exp,j}^{wo_vf}$ [Hz]	$f_{exp,j}^{w_vf}$ [Hz]	$\zeta_{exp,j}^{wo_vf}$ [%]	$\zeta_{exp,j}^{w_vf}$ [%]	$\Delta f_j^{wo_vf}$ [%]	$\Delta f_j^{w_vf}$ [%]	$MAC_j^{wo_vf}$ [-]	$MAC_j^{w_vf}$ [-]	Description
1	8.188	7.636	7.494	7.059	0.171	2.196	9.261	8.173	0.997	0.990	Vertical
2	11.056	10.118	10.157	9.382	0.293	1.797	8.851	7.844	0.904	0.992	Lateral
3	11.357	11.033	10.819	10.519	0.224	3.604	4.973	4.886	0.978	0.941	Torsion
4	20.042	19.436	19.627	18.115	0.513	2.187	2.114	7.292	0.995	0.995	Lateral
5	20.154	19.534	21.385	19.978	0.437	2.201	-5.756	-2.222	0.963	0.962	Longitudinal

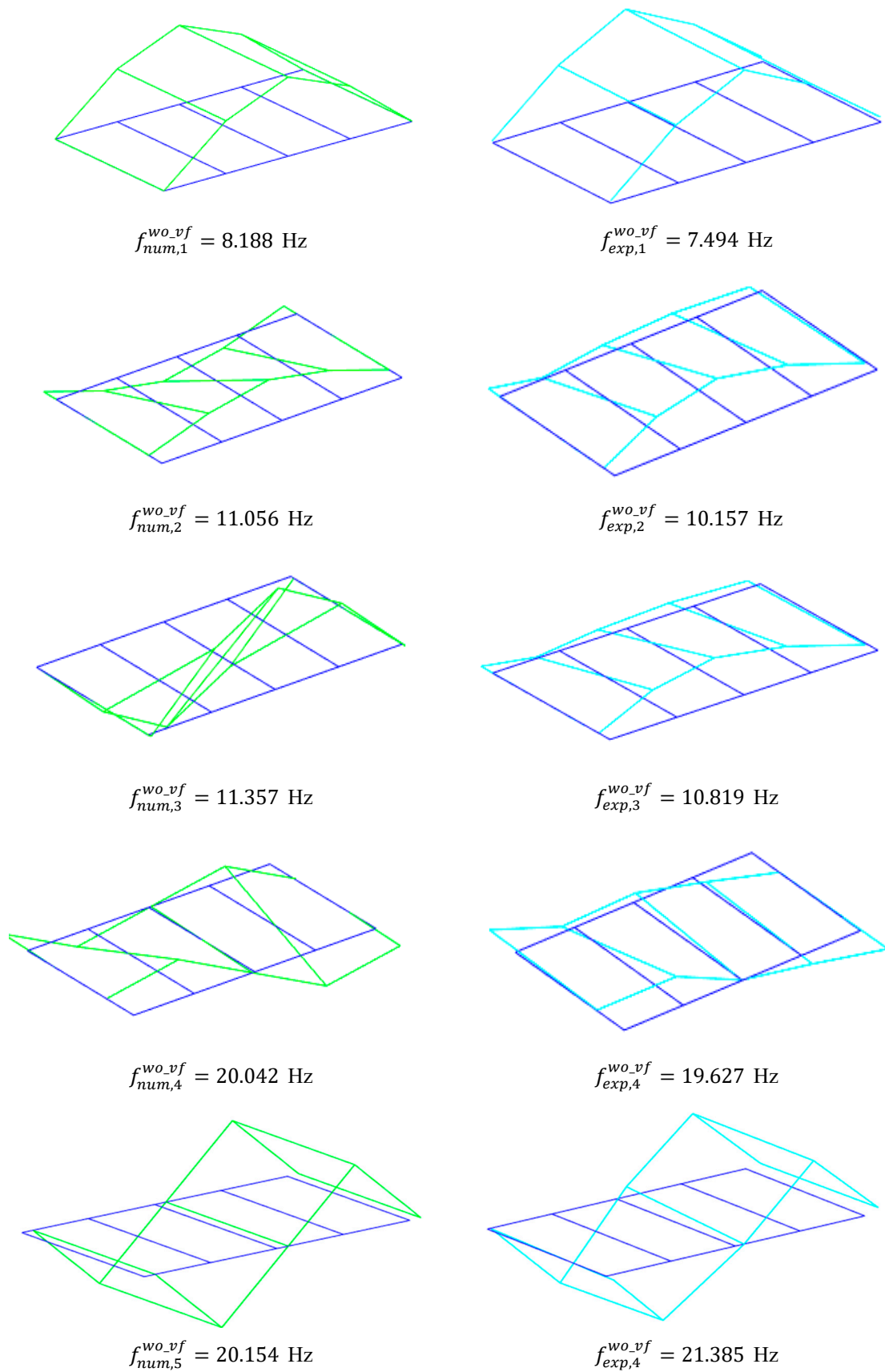


Figure 5. First five numerical, $\phi_{num,j}^{wo_vf}$, and experimental, $\phi_{exp,j}^{wo_vf}$, vibration modes of the laboratory footbridge without the vinyl flooring (being j the number of the considered vibration mode).

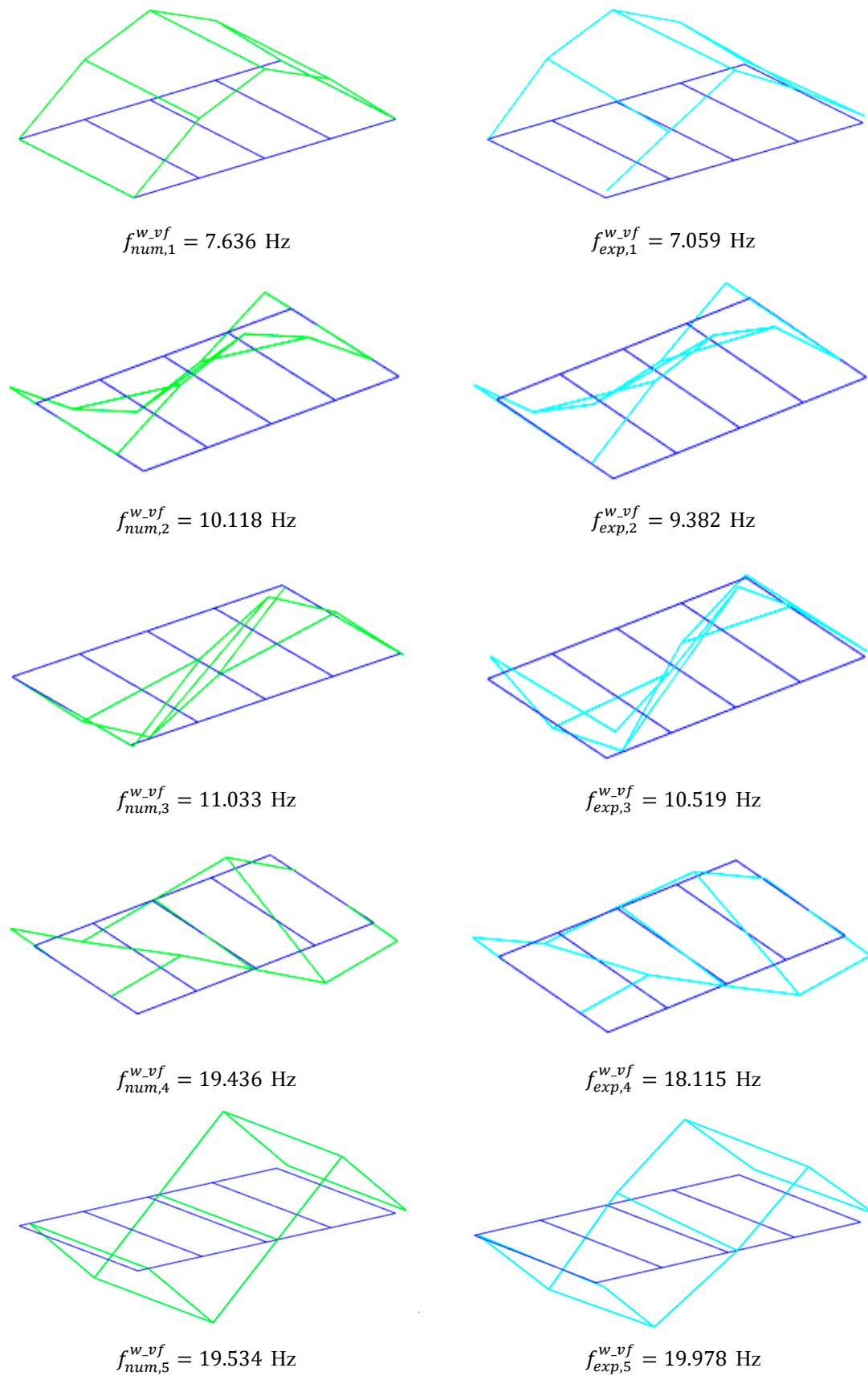


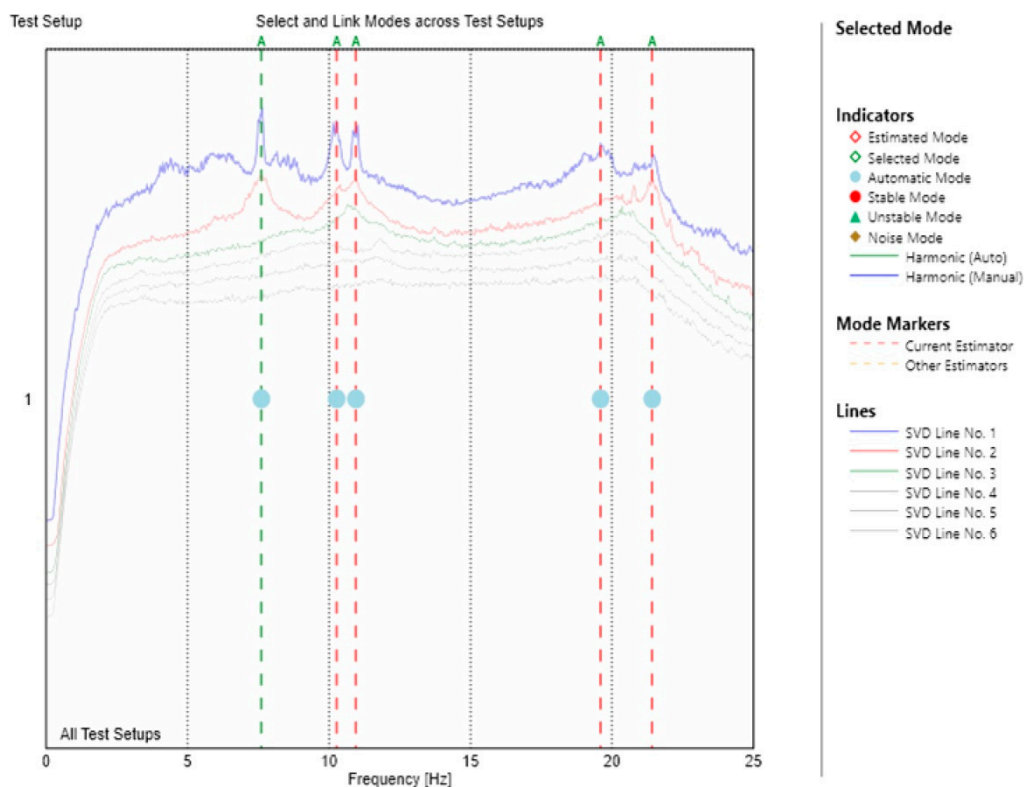
Figure 6. First five numerical, $(j\phi_{num,j}^{w,vf})$, and experimental, $\phi_{exp,j}^{w,vf}$, vibration modes of the laboratory footbridge with the vinyl flooring (being j the number of the considered vibration mode).

4.2. Experimental Identification of the Modal Parameters of the Laboratory Footbridge

Later, the modal parameters of the laboratory footbridge without and with the vinyl flooring were identified experimentally via the signal processing of the records obtained during the development of two independent AVTs. Both experimental tests were conducted under ambient conditions, where the laboratory footbridge without and with the vinyl flooring was only excited by ambient noise. The response of the structure under these conditions was measured along two gridlines located at the two longitudinal beams of the deck (Figure 4). A total of 2×5 points equally distributed along each longitudinal beam were instrumented. The previously mentioned three high sensitivity triaxial force balance accelerometers (Kinematics Episensor ES-T, Pasadena, United States) and the Kinematic Granite data acquisition system were used again. The accelerometers were connected to the structure via three screws. Two of these accelerometers were fixed as references, and the other one was moved successively to the different positions of the gridlines. An optimal sensor placement algorithm [24] was used to select the best location for the two reference accelerometers. Thus, the considered locations ensure the experimental identification of the first five vibration modes of the laboratory footbridge. Eight different set-ups were conducted during each AVT. A sampling frequency of 100 Hz and duration for each set-up of 600 s were considered for both experimental tests.

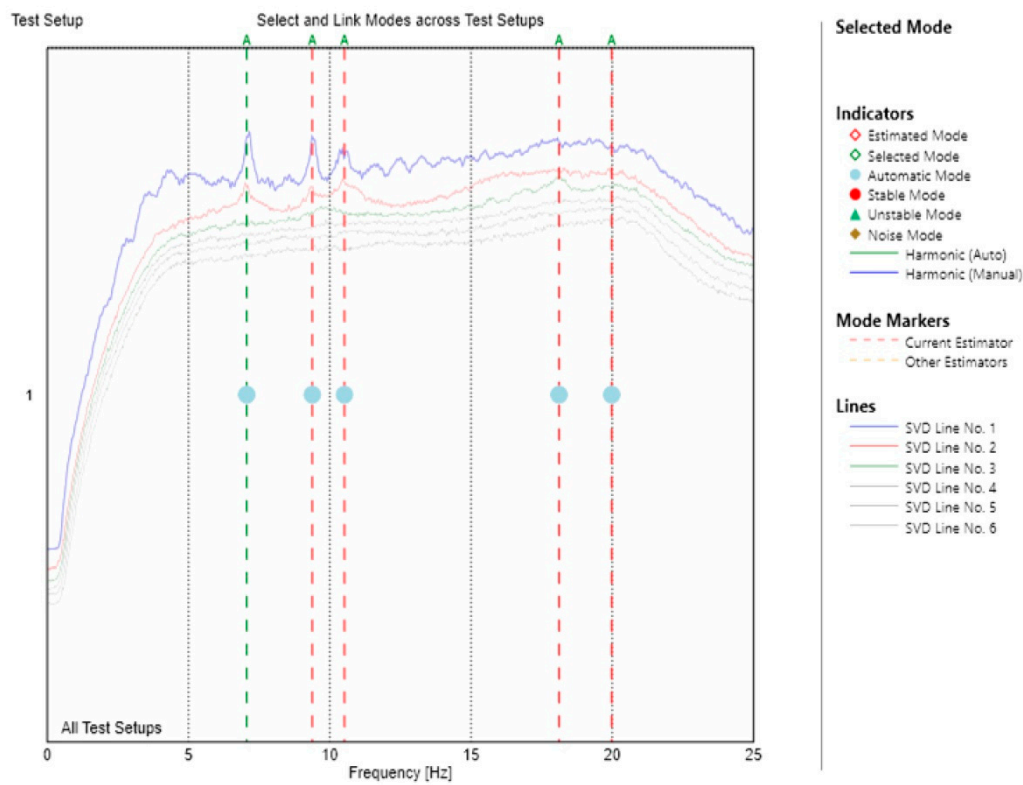
The experimental modal parameters of the footbridge were obtained via the signal processing of the records obtained during the development of each mentioned AVT. An OMA algorithm in time domain, the SSI algorithm [20] was used for this purpose as implemented in the software Artemis [26].

Figure 7 illustrates the singular values decomposition of the spectral densities for all the test set-ups and the experimental natural frequencies of the laboratory footbridge without and with the vinyl flooring according to the SSI algorithm [20].



(a)

Figure 7. Cont.



(b)

Figure 7. Singular values decomposition of the spectral densities for all the test set-ups and experimental natural frequencies identified by the stochastic subspace identification (SSI) algorithm for the laboratory footbridge: (a) without the vinyl flooring and (b) with the vinyl flooring [20].

Thus, the first five natural frequencies of the laboratory footbridge without, $f_{exp,j}^{wo_vf}$, and with, $f_{exp,j}^{w_vf}$, the vinyl flooring (being j the number of the considered vibration mode), and the associated vibration modes, $\phi_{exp,j}^{wo_vf}$, and $\phi_{exp,j}^{w_vf}$, were identified experimentally. Table 3 shows the first five experimental natural frequencies, $f_{exp,j}^{wo_vf}$ and $f_{exp,j}^{w_vf}$, and Figures 5 and 6 illustrate the first five experimental vibration modes of the laboratory footbridge, $\phi_{exp,j}^{wo_vf}$ and $\phi_{exp,j}^{w_vf}$.

Finally, the numerical and experimental natural frequencies and vibration modes of the laboratory footbridge without and with the vinyl flooring have been compared in Table 3. In order to validate the correlation between the numerical and experimental modal parameters both the relative differences, $\Delta f_j^{wo_vf}$ and $\Delta f_j^{w_vf}$ (being j the considered vibration mode), and the modal assurance criterion ratios, $MAC_j^{wo_vf}$ and $MAC_j^{w_vf}$, have been taken into account again. As Table 3 shows both the value of the experimental natural frequencies and associated vibration modes are in good agreement with the results obtained numerically. All the relative differences, $\Delta f_j^{wo_vf}$ and $\Delta f_j^{w_vf}$, are lower than 10% and all the MAC ratios, $MAC_j^{wo_vf}$ and $MAC_j^{w_vf}$, are greater than 0.90.

4.3. Discussion of the Results

In this manner, the non-structural damping ratios, $\zeta_{ns,j}$ (being j the number of the considered vibration mode), due to the vinyl flooring can be determined. Table 4 shows the non-structural damping ratios, $\zeta_{ns,j}$, for the five considered vibration modes. These non-structural damping ratios have been obtained by subtracting of the values of the experimental damping ratios of the footbridge without the vinyl flooring from the values of the experimental damping ratios of the footbridge with the vinyl flooring.

Table 4. Estimation of the non-structural damping ratios, $\zeta_{ns,j}$ [%], due to the vinyl flooring (being j the number of the considered vibration mode).

Modes	$\zeta_{exp,j}^{wo_vf}$ [%]	$\zeta_{exp,j}^{w_vf}$ [%]	$\zeta_{ns,j} = \zeta_{exp,j}^{w_vf} - \zeta_{exp,j}^{wo_vf}$ [%]	Description
1	0.171	2.196	2.025	Vertical
2	0.293	1.797	1.504	Lateral
3	0.224	3.604	3.380	Torsion
4	0.513	2.187	1.674	Lateral
5	0.437	2.201	1.764	Longitudinal

Finally, Figure 8 illustrates the variation of the experimental damping ratio of the laboratory footbridge without and with the vinyl flooring in terms of the considered vibration mode. The average experimental damping ratios of the footbridge without and with the vinyl flooring, 0.328 and 2.397% have been included in Figure 8 as references. The average non-structural damping ratio of 2.069% has also been obtained and included in Figure 8. At this point, two main results may be obtained from the analysis of Figure 8: (i) the effect of the vinyl flooring is greater on the damping ratios of the vertical and torsional vibration modes than on the lateral and longitudinal vibration modes and (ii) the effect on the damping ratios of all considered horizontal vibration modes, lateral and longitudinal, is similar.

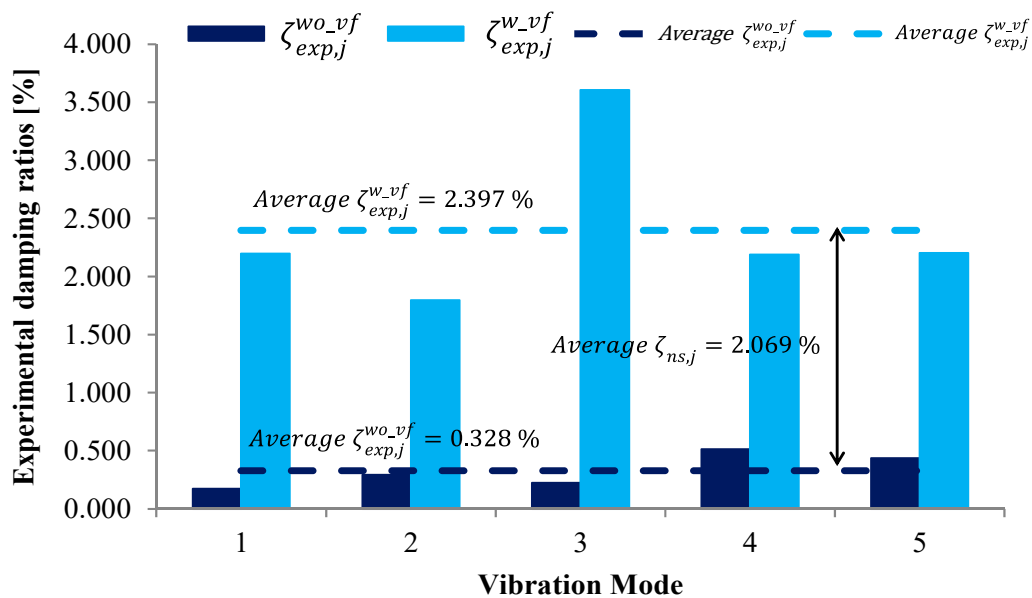


Figure 8. Variation of the experimental damping ratios [%] of the laboratory footbridge without and with the vinyl flooring.

According to these results, the vinyl flooring can be taken into account as a passive damping system in order to reduce the pedestrian-induced vibrations in steel footbridges. The effective implementation of this pavement allows increasing the damping ratios of steel footbridges with several advantages in comparison with the conventional external passive damping devices as, for instance, a smaller budget and a better integration with the aesthetics of the structure.

5. Conclusions

In this paper, the effect of vinyl flooring on the modal properties of steel footbridges has been analyzed. The Jorge Manrique footbridge is a bowstring arch structure located at Murcia (Spain). After its opening, users complained about several comfort problems of this structure. On the one hand, the floor of the footbridge, configured by a tempered glass layer, was a sliding surface which caused numerous pedestrian falls. On the other hand, pedestrian-induced vibrations problems were

denounced when the structure was occupied by a large number of pedestrians. In order to solve the first problem, a vinyl flooring was installed on the structure. The implementation of this non-structural element not only avoided successfully the pedestrian falls but also mitigated the pedestrian-induced vibrations problems. This side effect motivated the development of this study. Thus, as a first step, the modal parameters of the Jorge Manrique footbridge were identified experimentally. As result of this identification process, it was checked that although several natural frequencies of the footbridge were inside the frequency ranges which characterize several human rhythmic activities and a high pedestrian traffic usually crossed the structure, the high damping ratios obtained experimentally justify the absence of pedestrian-induced vibration problems. In order to quantify the influence of the vinyl flooring on these damping ratios, a comparative method was performed on a laboratory steel footbridge. As a result of this study, an average non-structural damping ratio of 2.069% was obtained for all the considered vibration modes. The results of this study show that this type of pavement can be considered as a valuable tool to be used as a passive damping system in order to control the response of steel footbridges under pedestrian action. Nevertheless, further studies are needed in order to better characterize the effect of vinyl flooring on other types of steel footbridges, to develop appropriate mathematical models which assist in predicting numerically the response of steel footbridges damped with this non-structural element and to analyze some possible limitations about the widespread use of vinyl flooring in outdoor scenarios.

Author Contributions: Conceptualization, J.F.J.-A. and A.S.; Methodology, J.F.J.-A.; Software, J.P.-A. and A.M.H.D.; Validation, J.F.J.-A. and A.S.; Writing-Original Draft Preparation, J.F.J.-A.; Writing-Review and Editing, A.S.; Funding Acquisition, A.S.

Funding: This work was partially funded by the Ministerio de Economía y Competitividad of Spain and the European Regional Development Fund under research project DPI2014-53947-R.

Acknowledgments: The authors extend their sincere appreciation to the civil engineers José Antonio Blanco Barquero (Murcia City Hall), José Rodríguez Segado (ATI-EPRON Corporation), Pedro J. Aranda González (ATI-EPRON Corporation) and Pedro de los Santos Jiménez Meseguer (Catholic University of Murcia) for their collaboration and helpful advices in the performance of the AVT of the Jorge Manrique footbridge.

Conflicts of Interest: The authors declare no conflict of interest.

References

- Zivanovic, S.; Pavic, A.; Reynolds, P. Vibration serviceability of footbridges under human-induced excitation: A literature review. *J. Sound. Vib.* **2005**, *279*, 1–74. [[CrossRef](#)]
- Caetano, E.; Cunha, A.; Wasoodev, H.; Raoul, J. *Footbridge Vibration Design*, 1st ed.; CRC Press Balkema: Leiden, The Netherlands, 2009.
- Dallard, P.; Fitzpatrick, A.J.; Le Bourva, S.; Low, A.; Smith, R.; Willford, M.; Flint, A. The London Millenium Footbridge. *Struct. Eng.* **2001**, *79*, 17–33.
- Dziuba, P.; Grillaud, G.; Flamand, O.; Sanquier, S.; Tétard, Y. La passerelle Solférino comportement dynamique. *Bull. Ouvrages Métalliques* **2001**, *1*, 34–57. (In French)
- Jiménez-Alonso, J.F.; Sáez, A. Motion-based optimum design of a slender steel footbridge and assessment of its dynamic behaviour. *Int. J. Steel Struct.* **2017**, *17*, 1459–1470. [[CrossRef](#)]
- Jiménez-Alonso, J.F.; Sáez, A. Controlling the Human-Induced Longitudinal Vibrations of a Nielsen-Truss Footbridge Via the Modification of its Natural Frequencies. *Int. J. Struct. Stab. Dyn.* **2017**, *17*, 1750061. [[CrossRef](#)]
- Oliveira, C.S. Fundamental Frequencies of Vibration of Footbridges in Portugal: From in Situ Measurements to Numerical Modelling. *Shock Vib.* **2014**, *2014*, 925437.
- Naranjo-Pérez, J.; Jiménez-Manfredi, J.; Jiménez-Alonso, J.F.; Sáez, A. Motion-Based Design of Passive Damping Devices to Mitigate Wind-Induced Vibrations in Stay Cables. *Vibration* **2018**, *1*, 269–289. [[CrossRef](#)]
- Shi, W.; Wang, L.; Lu, Z.; Zhang, Q. Application of an Artificial Fish Swarm Algorithm in an Optimum Tuned Mass Damper Design for a Pedestrian Bridge. *Appl. Sci.* **2018**, *8*, 175. [[CrossRef](#)]
- Soong, T.T.; Costantinou, M.C. *Passive and Active Control Structural Vibration Control in Civil Engineering*; State University of New York at Buffalo: Buffalo, NY, USA, 1994.

11. Rodriguez, V. La ciudad estrena la pasarela del ingeniero Calatrava. *La verdad* **1999**, *20*. (In Spanish)
12. Montesinos, M.J. Adiós a los resbalones. *La verdad*. 2012. Available online: <https://www.laverdad.es/murcia/v/20120809/murcia/adios-resbalones-20120809.html> (accessed on 26 March 2018).
13. Setra/AFGC. *Guide Méthodologique Passerelles Piétonnes*; Technical Guide Footbridges: Assessment of Vibration Behavior of Footbridge under Pedestrian Loading; Setra/AFGC: Paris, France, 2006.
14. Butz, C.H.; Heinemeyer, C.H.; Goldack, A.; Keil, A.; Lukic, M.; Caetano, E.; Cunha, A. *Advanced Load Models for Synchronous Pedestrian Excitation and Optimised Design Guidelines for Steel Footbridges (SYNPEx)*; Research Fund for Coal and Steel: Brussels, Belgium, 2007.
15. Qin, C.L.; Zhao, D.Y.; Bai, X.D.; Zhang, X.G.; Zhang, B.; Jin, Z.; Niu, H.J. Vibration damping properties of gradient polyurethane/vinyl ester resin interpenetrating polymer network. *Mater. Chem. Phys.* **2006**, *97*, 517–524. [[CrossRef](#)]
16. ABC. Atlas, Bilbao cubre con una alfombra antideslizante el Puente de Calatrava. 2010. Available online: <https://www.abc.es/20101221/espana/alfombra-puente-calatrava-201012211207.html> (accessed on 26 March 2018).
17. Devin, A.; Fanning, P.J.; Pavic, A. Modelling effect of non-structural partitions on floor modal properties. *Eng. Struct.* **2015**, *91*, 58–69. [[CrossRef](#)]
18. ASTM F1303-04(2014). *Standard Specification for Sheet Vinyl Floor Covering with Backing*; ASTM International: West Conshohocken, PA, USA, 2014.
19. Forbo Flooring Systems 2018. Available online: <http://www.forbo.com/> (accessed on 26 March 2018).
20. Magalhães, F.; Cunha, A. Explaining Operational Modal Analysis with data from an arch bridge. *Mech. Syst. Signal Process.* **2011**, *25*, 1431–1450. [[CrossRef](#)]
21. Midas FEA 2016. Available online: <http://en.midasuser.com/> (accessed on 7 May 2018).
22. Eurocode 3. *EN 1993-1-1: Design of Steel Structures: Part 1-1: General Rules and Rules for Buildings*; European Committee for Standardisation: Brussels, Belgium, 2005.
23. Clough, R.; Penzien, J. *Dynamic of Structures*; McGraw-Hill, Inc.: New York, NY, USA, 1993.
24. Sun, H.; Büyüköztürk, O. Optimal sensor placement in structural health monitoring using discrete optimization. *Smart Mater. Struct.* **2015**, *24*, 1–16. [[CrossRef](#)]
25. Magalhães, F.; Cunha, A.; Caetano, E.; Brincker, R. Damping estimation using free decays and ambient vibration tests. *Mech. Syst. Signal Process.* **2010**, *24*, 1274–1290.
26. ARTeMIS Modal Pro. 2016. Available online: <http://www.svibs.com/> (accessed on 7 May 2018).
27. Zivanovic, S.; Pavic, A.; Reynolds, P. Finite element modelling and updating of a lively footbridge: The complete process. *Eng. Struct.* **2007**, *301*, 126–145.
28. Van Nimmen, K.; Lombaert, G.; De Roeck, G.; Van den Broeck, P. Vibration serviceability of footbridges: Evaluation of the current codes of practice. *Eng. Struct.* **2014**, *59*, 448–461. [[CrossRef](#)]
29. Connor, J. *Introduction to Structural Motion Control*; Prentice Hall. Pearson Education, Inc.: Upper Saddle River, NJ, USA, 2003.
30. Akay, A.; Carcaterra, A. Damping Mechanisms. In *Book Active and Passive Vibration Control of Structures*, 1st ed.; Hagedorn, P., Spelsberg-Korspeter, G., Eds.; CISM International Centre for Mechanical Sciences: Vienna, Austria, 2014; Volume 558, pp. 259–299.
31. Adhikari, S. Damping Models for Structural Vibration. Ph.D. Thesis, University of Cambridge, Cambridge, UK, 2000.
32. Eurocode 1. *EN 1991-1-4: Actions on Structures-General Actions—Part. 1-4: Wind Actions*; European Committee for Standardisation: Brussels, Belgium, 2004.

